APPLIED SPECTROSCOPY REVIEWS
Vol. 39, No. 3, pp. 365–384, 2004

# Internal Reflection and ATR Spectroscopy

**Milan Milosevic***

Harrick Scientific Corporation, Ossining, New York, USA

## CONTENTS

ABSTRACT . . . . . . . . . . . . . . . . . . . . . . . . . . . 366

I. INTRODUCTION . . . . . . . . . . . . . . . . . . . . . . . . . 366

II. THEORY OF ATR SPECTROSCOPY . . . . . . . . . . . . 367
A. Reflectance Formula . . . . . . . . . . . . . . . . . . . . . 367
B. The Evanescent Wave . . . . . . . . . . . . . . . . . . . . 369
C. Subcritical and Supercritical Reflection . . . . . . . . . 374

III. ADVANCED ASPECTS OF ATR SPECTROSCOPY . . . 375
A. Depth Profiling Using Variable Angle ATR Spectroscopy . . . . . . . . . . . . . . . . . . . . . . . . . 375
B. Orientation Studies Using Polarized Variable Angle ATR . . . . . . . . . . . . . . . . . . . . . . . . . . . . 376
C. ATR Microsampling . . . . . . . . . . . . . . . . . . . . . 377

*Correspondence: Milan Milosevic, Harrick Scientific Corporation, Ossining, NY 10562, USA; E-mail: info@harricksci.com.



DOI: 10.1081/ASR-200030195 0570-4928 (Print); 1520-569X (Online)
Copyright © 2004 by Marcel Dekker, Inc. www.dekker.com

Request Permissions / Order Reprints
powered by RIGHTSLINK COPYRIGHT CLEARANCE CENTER, INC.

D. ATR in Process Control and Reaction Monitoring . . . 379
E. Grazing Angle ATR . . . . . . . . . . . . . . . . . . . . . 379

IV. ACCESSORIES FOR ATR SPECTROSCOPY . . . . . . . 380

V. CONCLUSION . . . . . . . . . . . . . . . . . . . . . . . . . . 383

ACKNOWLEDGMENTS . . . . . . . . . . . . . . . . . . . . . 383

REFERENCES . . . . . . . . . . . . . . . . . . . . . . . . . . 383

## ABSTRACT

The connection between ATR spectroscopy and the physical phenomena of internal reflection and evanescent wave is reviewed. In this context advanced aspects of ATR spectroscopy are discussed. A brief review of the accessories used for ATR measurements is given along with a cursory review of general strategies for their incorporation into FTIR spectrometers.

*Key Words:* ATR spectroscopy; Internal reflection; Reflectance; Fresnel equations; Evanescent wave.

## I. INTRODUCTION

A variety of spectroscopic techniques are necessary due to the wide range of samples that are usually investigated. The selection of the appropriate technique minimizes the need for elaborate sample preparations and simplifies data analyses. Typically, gaseous samples are best suited to analysis by transmission, liquids by transmission or attenuated total reflection (ATR) (also known as internal reflection), and powders by ATR or diffuse reflectance. Transmission spectroscopy was once the dominant spectroscopic technique, a standard against which all other spectroscopic techniques were compared. In the area of infrared (IR) spectroscopy, however, ATR has taken over for all but gaseous samples.

It is my intent to review the physical phenomenon of internal reflection and how it is utilized in ATR spectroscopy. Many advanced aspects of ATR, such as depth profiling or orientation studies, are built on particular features of reflectance. The beauty of ATR is that the reflectance, as a physical property of an interface, is a well-understood phenomenon. Exact description

of reflectance is given by Fresnel equations. Thus, providing the input parameters for the Fresnel equations are known, the reflectance of an interface can be calculated exactly. Similarly, the laws of transmission of light through a medium are known. Nevertheless, the richness of the phenomena described by these laws never ceases to surprise us.

In Section II, we briefly review the reflectance formulae, the phenomenon of evanescent wave, and discuss the two domains of internal reflection. The later is important since the enormity of the difference between the two modes of internal reflection is rarely sufficiently emphasized and is generally under-appreciated. The concepts developed are then utilized to discuss the more advanced aspects of ATR spectroscopy.

## II. THEORY OF ATR SPECTROSCOPY

### A. Reflectance Formula

Light striking an interface is partially transmitted and partially reflected. The transmitted component is refracted at the interface. The angle of refraction is related to the angle of incidence by Snell's Law:

$$n_0 \sin\theta = n_s \sin\varphi \tag{1}$$

Here, $n_0$ is the refractive index of the incident material, $\theta$ is the angle of incidence, $n_s$ is the refractive index of the second material, and $\varphi$ is the angle of refraction into the second medium.

Despite the fact that they both follow from the same equation, the two types of reflection from an interface are, in spectroscopy, generally treated as two different phenomena. If the refractive index of the medium from which the light is incident onto the interface ($n_0$) is higher than that of the second medium ($n_s$), the reflection is called internal. In the opposite case, i.e., $n_0 < n_s$, the reflection is called external. For the external reflection, the angle of refraction is always smaller than the angle of incidence, i.e., $\phi < \theta$.

The reflectance of an interface between two materials is described by Fresnel equations.[1] Two polarizations of radiation reflect differently:

$$r_s = -\frac{\sin(\theta - \varphi)}{\sin(\theta + \varphi)} \tag{2}$$

$$r_p = -\frac{\tan(\theta - \varphi)}{\tan(\theta + \varphi)} \tag{3}$$

These Fresnel amplitude coefficients specify the electric field amplitudes and phases of the reflected radiation as functions of incident angle, polarization,

amplitude of the electric field of the incident radiation, and the complex refractive indices of the two materials.

There is a fundamental symmetry between external and internal reflections. The reflectance coefficients are the same for the two cases if the corresponding angles of incidence form a Snell pair (i.e., they are related through Snell's Law). In this case, the external reflectance coefficients are the same, except for the overall sign, as the internal reflectance coefficients for all incident angles. First, consider light impinging on the interface from the rarer medium. Since the angles in the optically rarer medium are always larger than their Snell counterparts in the optically thicker medium, there is a maximum angle of refraction that corresponds to the incident angle of $90^\circ$ (i.e., the largest possible angle of incidence). All angles of refraction are between zero and this maximum angle of refraction. Angles larger than this maximum angle of refraction are not possible.

Now consider the other case, where the incident radiation originates from the higher refractive index medium. At incident angles corresponding to the angles of refraction less than $90^\circ$, the reflectance behavior is similar to that of the external reflectance case described before, i.e., the light is refracted through the interface. However, the incident angle can be increased beyond the maximum angle of refraction, so all the incident rays are reflected within the higher refractive index medium. The incident angle at which the light is no longer refracted is called the critical angle. Thus, in the case, where the light is impinging on the interface from the higher refractive index medium, there are two distinct domains. One is the subcritical domain and the other, the supercritical domain, which is known as the region of ATR.

Incorporating Snell's Law (1) into the equations for the amplitude coefficients (2) and (3) in order to eliminate the angle of refraction gives expressions for amplitude coefficients containing only material parameters and incident geometry:

$$r_{\mathrm{s}} = -\frac{n_0 \cos\theta - \sqrt{n_{\mathrm{s}}^2 - n_0^2 \sin^2\theta}}{n_0 \cos\theta + \sqrt{n_{\mathrm{s}}^2 - n_0^2 \sin^2\theta}} \tag{4}$$

$$r_{\mathrm{p}} = \frac{(n_{\mathrm{s}}^2/n_0)\cos\theta - \sqrt{n_{\mathrm{s}}^2 - n_0^2 \sin^2\theta}}{(n_{\mathrm{s}}^2/n_0)\cos\theta + \sqrt{n_{\mathrm{s}}^2 - n_0^2 \sin^2\theta}} \tag{5}$$

This new form of Eqs. (2) and (3), unlike the original expression, remains meaningful both for the supercritical domain of internal reflection and for complex refractive indices. Although the most general case of both media

being absorptive is readily handled by Eqs. (4) and (5), only the case of a non-absorbing incident medium (i.e., $n_0$ real) is of practical interest. The complex refractive index $n_s$ can be written in terms of the real and imaginary parts as:

$$n_s = n + i\kappa \tag{6}$$

where $n$ and $\kappa$ are the index of refraction and the index of absorption, respectively. First, we see that, in the case in which a sample is non-absorbing ($\kappa = 0$), the square root term vanishes for the angle $\theta_c$ for which:

$$n_s = n_0 \sin \theta_c \tag{7}$$

A comparison of Eq. (7) with Snell's Law (1) reveals that the critical angle $\theta_c$ is also the critical angle for internal reflection since for this angle of incidence, the angle of refraction $\varphi$ is exactly $90^\circ$ ($\sin \varphi = 1$). If the angle of incidence is greater than the critical angle, the expression under the square root becomes negative and the square root becomes imaginary. As a result, the Fresnel reflection coefficients (4) and (5) become complex numbers with a modulus of one. Thus, the reflectance of the interface, which is the square of the absolute value of a Fresnel coefficient, becomes total (i.e., 1 or 100%). The fact that the reflectance of the interface becomes total in the supercritical regime of internal reflection could be taken as an indication that there is no electromagnetic field beyond the interface. However, in the case of supercritical internal reflection, a very special kind of electromagnetic field, called the evanescent wave, is established beyond the interface.

## B. The Evanescent Wave

To understand the evanescent wave, which can be seen as a remnant of a transmitted (refracted) wave as the angle of incidence exceeds the critical angle, let us examine the electric field of the transmitted wave. Following the geometry shown in Fig. 1, the electric field of the transmitted wave is:

$$\mathbf{E}_t(\mathbf{r},\ t) = \mathbf{E}_t(0,\ t)e^{in_s\mathbf{k}_t\mathbf{r}} \tag{8}$$

where $\mathbf{k}_t$ is the wave vector of the transmitted wave, $\mathbf{r}$ is the radius vector of the position in which we are observing the field, and the interface is in the $x$–$y$ plane. The exponent of the oscillatory factor in Eq. (8) is a scalar product that can be shown as a sum of three terms:

$$\mathbf{k}_t\mathbf{r} = (k_t)_x x + (k_t)_y y + (k_t)_z z \tag{9}$$

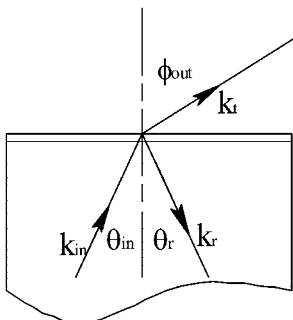


***Figure 1.*** Geometry of reflection.

The $x$ and $y$ terms in Eq. (9) represent oscillatory propagation in the $x$–$y$ plane (parallel to the interface). The $z$ term can be rewritten as:

$$n_s(k_t)_z = n_s k \cos\varphi = k\sqrt{n_s^2 - n_0^2\sin^2\theta} \tag{10}$$

Note that the term $\cos\varphi$ is only meaningful in the regime of subcritical internal reflection. The use of Snell's Law helps in extending the meaning of expression (10) to the regime of supercritical internal reflection. Expression (10) is the crucial expression for understanding supercritical reflection and hence ATR or internal reflection spectroscopy. For the angles of incidence smaller than critical, the expression under the square root in Eq. (10) is positive and hence the square root is a real number. Thus, the propagation along the $z$-axis is oscillatory and the expression describes the transmitted (refracted) radiation. As the angle of incidence exceeds the critical value, the expression under the square root becomes negative and the term becomes imaginary. This radically changes the nature of the electromagnetic field behind the interface. Expression (8) becomes:

$$\mathbf{E}(x,\ y,\ z,\ t) = \mathbf{E}(0,\ 0,\ 0,\ t)e^{i(k_x x + k_y y)}e^{-k_z\sqrt{n_0^2\sin^2\theta - n_s^2}} \tag{11}$$

Expression (11) describes the evanescent wave that propagates along the interface ($x$–$y$ plane). The magnitudes of the electric and magnetic field of the evanescent wave decrease exponentially away from the interface.

It is important to note that the evanescent wave is a propagating electromagnetic wave bound to the interface. This wave is, due to the presence of the exponentially decaying factor, known as inhomogeneous.[1] There is a peculiar property associated with the evanescent wave; i.e., it is not transversal. As a rule, the electric and the magnetic field of an electromagnetic wave are perpendicular to the direction of propagation. Hence, there is no field

component (neither electric nor magnetic) along the direction of propagation, i.e., the mutually perpendicular electric and magnetic fields of the electromagnetic wave are also perpendicular to the direction of propagation. This is a reflection of the fact that the photon is without mass. Thus, it comes as a surprise that this transversality, generally, does not hold for the evanescent wave. The evanescent wave induced by the s-polarized incident light is still transversal. The electric field is parallel to the totally reflecting interface, but perpendicular to the direction of propagation (which is along the interface). However, p-polarized incident wave produces an evanescent wave with an electric field that has a component perpendicular to the interface (and to the direction of propagation) and a component parallel to the interface, thus along the direction of propagation. At a point in the interface, the electric field of the p-polarized evanescent wave oscillates in the plane of incidence between the transversal and longitudinal components that are mutually $90^\circ$ out of phase. The longitudinal component of the electric field vanishes at the critical angle. This enables an experimental setup in which the electric field of the evanescent wave is chosen to selectively probe a particular direction in the sample of interest. If the sample is anisotropic, properties of the sample in three perpendicular directions can be independently analyzed. For probing the direction in the sample perpendicular to the interface, it is important to select the angle of incidence just above critical in order to minimize the longitudinal component.

One can find the characteristic distance $d_\mathrm{p}$ at which the field strength falls off to $1/\mathrm{e}$ of its value at the interface (also known as penetration depth):

$$d_\mathrm{p} = \frac{\lambda}{2\pi\sqrt{n_0^2 \sin^2\theta - n_\mathrm{s}^2}} \tag{12}$$

where $\lambda$ is the wavelength of light.

In general, the sample absorbs, hence $n_\mathrm{s}$ is complex. The real and imaginary parts of the complex refractive index (6) are known as the optical constants of the material. If $n_\mathrm{s}$ is known, expressions (4) and (5) can be used to calculate the reflectances for the two polarizations exactly. While straightforward, the explicit general expression for the reflectance is very complicated and not particularly illuminating. The complexity of this expression was one of the original motivations for Harrick[2] to introduce the weak absorption limit. By simplifying the expressions (4) and (5) to the weak absorption form (i.e., $\kappa \ll 1$), the roles of various parameters figuring in the equations become more transparent. One can formally arrive at the low absorption limit expressions by retaining in Eqs. (4) and (5) only terms linear in $\kappa$. There is, however, a more revealing approach to arriving at those expressions.

Propagation of light through a homogeneous medium is easily understood within the framework of Maxwell's theory.[1] The solution to Maxwell's equations is a plane wave of the form given in Eq. (8). If the direction of propagation is along the $x$-axis, the expression simplifies to:

$$\mathbf{E}(x,\ t) = \mathbf{E}(0,\ t)\mathrm{e}^{\mathrm{i}nkx}\mathrm{e}^{-\kappa kx} \tag{13}$$

and since the radiation intensity $I(x)$ is proportional to the square of absolute value of the amplitude:

$$I(x) = I(0)\mathrm{e}^{-2\kappa kx} \tag{14}$$

It is customary to introduce the absorption coefficient as:

$$\alpha(k) = 2\kappa k \tag{15}$$

With the substitution of Eq. (15), Eq. (14) becomes:

$$I(x) = I(0)\mathrm{e}^{-\alpha x} \tag{16}$$

or, in differential form:

$$\frac{dI(x)}{dx} = -\alpha I(x) \tag{17}$$

This is also known as Lambert–Bouguer law. This law can be recast into a form that is more applicable to deriving the reflectance law in the low absorption limit. First, note that the radiation intensity $I(x)$ is proportional to the square of the field amplitude [hence, to the energy density of the electromagnetic field $u(\boldsymbol{r}, t)$] and the speed of light in the medium of propagation $c/n_{\mathrm{s}}$:

$$I(x) = u(\mathbf{r},\ t)\frac{c}{n_{\mathrm{s}}} \tag{18}$$

The path differential $dx$ can be expressed as:

$$dx = \frac{c}{n_{\mathrm{s}}}\,dt \tag{19}$$

Equation (17) can then be rewritten as:

$$\frac{du(\mathbf{r}, t)}{dt} = -\frac{c}{n_{\mathrm{s}}}\alpha u(\mathbf{r},\ t) \tag{20}$$

Expression (20) describes light absorption in unit volume per unit time rather than per unit length.

Let us analyze reflected radiation in the regime of supercritical internal reflection. Obviously, in the absence of transmitted (i.e., refracted) radiation, the reflected radiation is the incident radiation less the radiation absorbed by

the sample. Assume that the incoming radiation is a collimated beam of a cross-section $A_0$ incident at an angle $\theta$. The area of the interface illuminated by the incoming beam is $A_0/\cos\theta$. The energy $U_a$ absorbed per unit time (i.e., the absorbed power) is:

$$\frac{dU_a}{dt} = \int dV \frac{du}{dt} \tag{21}$$

where the volume of integration extends over the entire space occupied by the sample. Expression (21) simply restates the definition of energy density $u = dU/dV$. However, by inserting Eq. (20) into Eq. (21), and by recalling that:

$$u = \frac{|\mathbf{E}_t(x, y, z, t)|^2}{4\pi} = \frac{|\mathbf{E}_{t0}|^2 e^{2z/d_p}}{4\pi} \tag{22}$$

one obtains:

$$\frac{dU_a}{dt} = -\frac{cA_0}{4\pi n_s \cos\theta} \alpha |\mathbf{E}_{t0}|^2 \frac{d_p}{2} \tag{23}$$

where $\mathbf{E}_{t0}$ is the vector of the electric field at the interface from the sample side. The field $\mathbf{E}_{t0}$ is connected to the incoming field $\mathbf{E}_0$ via the Fresnel transmission coefficient $t_{1,2}^{s,p}$,[1]

$$\mathbf{E}_{t0}^{s,p} = t_{1,2}^{s,p} \mathbf{E}_0^{s,p} \tag{24}$$

where the superscripts s and p stand for the different polarizations of the incident light and the subscripts 1, 2 indicate that the light is incident from medium 1 and transmitting into medium 2. If we note that the total power of the incoming beam is:

$$P_{in} = \frac{cA_0}{4\pi n_0} |\mathbf{E}_0|^2 \tag{25}$$

then, employing Eqs. (23) and (24), the absorbed power becomes:

$$P_a^{s,p} = \frac{n_0}{n\cos\theta} \alpha |t_{1,2}^{s,p}|^2 \frac{d_p}{2} P_{in} \tag{26}$$

Since the reflected radiation is incoming radiation less the absorbed radiation:

$$R^{s,p} = 1 - \frac{n_0 \alpha |t_{1,2}^{s,p}|^2 d_p}{2n\cos\theta} \tag{27}$$

Equation (27) is exactly the expression we find by simplifying the exact expressions (4) and (5) to a low absorption limit. However, this derivation of Eq. (27) illuminates the process of supercritical internal reflection by

highlighting the mechanism of absorption. Note that in deriving Eq. (23), we used the expression for the evanescent wave for the case where the rarer medium is non-absorbing (i.e., $\kappa = 0$). Hence, Eq. (27) is correct only to linear terms in absorption index.

### C. Subcritical and Supercritical Reflection

The low absorption limit can be utilized to explicitly demonstrate the difference between the subcritical internal (equivalent to external) and supercritical internal reflection. Keeping the lowest non-vanishing term in $\kappa$ for subcritical internal reflection gives:

$$R_i(\kappa) = R_i(0) + b_i\kappa^2 \tag{28}$$

where the index $i$ stands for either of the two different polarizations s or p, and the coefficient $b_i$ is a function of the refractive indices and the angle of incidence. The equivalent expression for the supercritical internal reflection is:

$$R_i(\kappa) = 1 - \beta_i\kappa \tag{29}$$

where index $i$ again stands for different polarizations and the coefficient $\beta_i$ is a function of the refractive indices and the angle of incidence. Expressions (28) and (29) make evident the drastic change in the nature of reflectance that occurs at the critical angle. The subcritical reflectance (28) has a quadratic dependence on $\kappa$ and is thus essentially insensitive to the weak absorption index. Hence, subcritical reflectance is dominated by the real part of the refractive index. Supercritical reflectance (29) is, on the other hand, dominated by the absorption index $\kappa$. The expression (29) for supercritical reflectance is similar to the expression for transmittance in the weak absorption limit:

$$\frac{T(\kappa)}{T(0)} = 1 - 4\pi k\kappa d \tag{30}$$

where $k = 1/\lambda$, and $d$ is the thickness of the sample. The fundamental similarity of the two expressions eased the original introduction of ATR spectroscopy. In both cases, a negative logarithm (absorbance transform) of the measured spectroscopic observable is proportional to the absorption index. However, while for the transmission measurement, this linear dependence continues to hold even for high absorbances, the linearity in the case of ATR breaks down with the increasing strength of the absorbance. Note that, in the case of transmittance, the wavenumber $k$ figures in as an explicit factor. This causes absorbance transform of the transmittance spectrum to be artificially enhanced at shorter wavelengths (i.e., higher wavenumbers).

Equations (29) and (30) demonstrate explicitly why supercritical internal reflection is useful for spectroscopy and why the usefulness of subcritical internal reflection (and hence external reflection) is generally limited. This is not to say that useful information cannot be extracted from subcritical (and external) reflectance spectra. However, the analysis is much less straightforward.

## III. ADVANCED ASPECTS OF ATR SPECTROSCOPY

### A. Depth Profiling Using Variable Angle ATR Spectroscopy

As soon as Harrick wrote his penetration depth expression, it became clear that controlling the angle of incidence controls the depth of penetration of the evanescent wave into the sample. With samples that are chemically different on the surface than in the bulk, spectra obtained at two different angles (thus two different penetrations) can be compared to deduce information on different chemical compositions between the surface and the bulk of the sample. To analyze this explicitly, let us combine Eqs. 20–22:

$$\frac{dU_{\mathrm{a}}}{dt} = -\frac{c}{4\pi n}|\mathbf{E}_{\mathrm{t0}}|^2 \int dV \alpha(z) \mathrm{e}^{-2z/d_{\mathrm{p}}} \qquad (31)$$

Note that, in the above expression, the implicit assumption was made that expression (22), valid in the case of a homogeneous non-absorbing sample, would approximately hold in the case the sample is both absorbing and inhomogeneous. We would expect though that expression (31) is approximately correct for a weakly absorbing sample i.e., $\kappa \ll 1$ whose real part of the refractive index is relatively uniform within the penetration depth. Under those conditions, Eq. (31) expresses the energy absorbed by the sample per unit time as a sum (integral) of absorptions by layers of the sample at different depths. The integral in Eq. (31) is a function of penetration depth $d_{\mathrm{p}}$. Strictly speaking, the integral on the RHS of Eq. (31) represents the Laplace transform of an absorption coefficient $\alpha(z)$. Mathematically, the inverse transform exists and it is unique, but the value of the integral must be known for all the values of $d_{\mathrm{p}}$ from zero to infinity.

Note that for a uniform sample the above integral becomes $\alpha d_{\mathrm{p}}/2$. If thus in expression (27) we replace $\alpha d_{\mathrm{p}}/2$ with the above integral, we obtain that for a non-uniform sample the reflectance becomes:

$$R^{\mathrm{s,p}}(d_{\mathrm{p}}) = 1 - \frac{n_0|t_{1,2}^{\mathrm{s,p}}|^2}{n\cos\theta}\int_0^{\infty} dz\alpha(z)\mathrm{e}^{-2z/d_{\mathrm{p}}} \qquad (32)$$

We can calculate the above integral for a simple case where the sample absorption coefficient is constant up to sample depth $t$ and is non-absorbing thereafter.

The result is:

$$R^{s,p}(d_p,\ t) = 1 - \frac{n_0 |t_{1,2}^{s,p}|^2 \alpha}{n \cos\theta} \int_0^t dz e^{-2z/d_p}$$
$$= 1 - \frac{n_0 |t_{1,2}^{s,p}|^2 \alpha d_p}{2n \cos\theta}(1 - e^{-2t/d_p}) \quad (33)$$

As expected, for $t = 0$ the reflectance is total (hence no absorption), and approaches result (27) as the thickness of the absorbing layer $t$ becomes much larger than the penetration depth $d_p$. In addition, in the case for which the film thickness is much smaller than the penetration depth, the absorbance is linearly proportional to the film thickness.

For a sample whose surface is chemically different from the bulk, it is possible to record a series of spectra at various angles of incidence (hence spanning a range of penetration depths) and from them to extract information on the chemical composition of the sample as a function of depth $t$. These types of studies are referred to as depth profiling studies. It is evident from Eq. (32) that depth profiling is limited to depths of approximately $d_p$.

The accessory that enables variable angle ATR (as well as specular reflection) studies to be routinely performed on a wide array of samples is Harrick's Seagull.[3]

## B. Orientation Studies Using Polarized Variable Angle ATR

As I have already mentioned in the discussion of the properties of the evanescent wave, the orientation of the electric field vector of the evanescent wave can be controlled using a polarizer and/or by changing the angle of incidence of the incident light. Let the plane of incidence be the $x-z$ plane with the $z$-axis perpendicular to the interface. The $y$-axis is then in the plane of interface and perpendicular to the plane of incidence. If the incident light is s-polarized, the electric field vector of the evanescent wave is along the $y$-axis. Thus, only molecular bonds with dipoles that have components along the $y$-axis can be excited by this evanescent wave. Assume that a sample has dipoles associated with a particular chemical bond all oriented along the $x$-axis. The above-described evanescent wave would not exhibit the absorption band associated with that bond in this orientation. However, if that sample is rotated in the $x-y$ plane by 90°, the absorption band appears in full strength. Therefore, a

measurement exhibiting this behavior would indicate an extraordinary degree of molecular orientation associated with that particular chemical bond. By rotating the sample by some angle $\alpha$ other than 90° would cause the strength of the bond to be proportional to $\sin^2(\alpha)$. If the incident light were p-polarized, the electric field vector would, as mentioned before, exhibit the particularly unusual behavior associated with inhomogeneous waves having the electric field component both parallel and perpendicular to the direction of propagation oscillating completely out of phase. Thus, there is a component of the electric field along the $x$-axis as well as the $z$-axis and contribution from both the $x$- and the $z$-components of bonds are always mixed together. By changing the angle of incidence, the relative strength of $x$-component and $z$-component can be changed in a controlled manner. Since, by rotating the sample 90° in the $x-y$ plane, the roles of the $x$- and $y$-directions in the sample can be exchanged, the $x$-component of bonds could be independently measured (by rotating the sample 90° and switching to the s-polarized light). This absorption bands associated with the $x$-components of bonds can be subtracted from the mixture of $x$- and $z$-component bands measured with p-polarized light. This enables that all three directions in the sample be independently probed and the orientation of chemical bonds in the sample evaluated. To enable routine measurements of oriented samples, Harrick provides the Ming-Sung attachment for its Seagull[3] accessory that enables continuous rotation of the sample in the plane of interface.

## C. ATR Microsampling

Prior to the introduction of Harrick's SplitPea accessory,[4] ATR spectroscopy was almost completely dominated by the multiple ATR technique. At the same time with the introduction of the SplitPea accessory, Spectra-Tech introduced an ATR objective for their FTIR microscopes.[5] The unchallenged reign of multiple ATR began to yield to the newly rediscovered technique of single reflection ATR. It soon began to be realized that, what was before considered a lack of sensitivity of ATR to all kinds of solid samples, was actually a result of poor contact between the sample and the ATR element. The small hot spot of the SplitPea and, even more, that of the ATR objective, for the most part rendered the issue of good sample-ATR element contact mute. For irregular solid samples, the benefit of a small hot spot could be best understood as follows. Assume that the sample is a hard polymer sphere such as a Teflon sphere. To get an ATR spectrum of the sphere, one needs to press the sphere against the sampling surface of the ATR element and locally deform it, so that the sphere and the ATR element are in direct physical contact over a circular spot of radius $r_0$.

To avoid stray light, the size of the contact area has to be equal to, or larger than, the size of the hot spot. The pressure distribution over the contacted area has the maximum in the center of the contact circle and vanishes at the edges. The radius of the contact circle grows with increased force on the sphere. The mechanical problem of an elastic sphere in contact with a hard plane is well understood and is known under the name of "Hertz contact problem." The expressions relating the radius of the contact circle, applied force, and the maximum pressure (that occurs in the center of the contact circle) are:

$$r_0 = \left[\frac{3}{2}FR\frac{1-\nu^2}{E}\right]^{1/3} \tag{34}$$

$$p_0 = \frac{3F}{2\pi r_0^2} \tag{35}$$

where $R$ is the radius of the sphere, $E$ and $\nu$ are the Young modulus and the Poisson ratio, $F$ is the applied force, and $p_0$ is the pressure in the center of the contact circle. Equations (34) and (35) can be combined to express $p_0$ in terms of the radius of the contacting circle:

$$p_0 = \frac{Er_0}{\pi R(1-\nu^2)} \tag{36}$$

In order to avoid damaging the surface of the ATR element, this pressure must always be smaller than the modulus of rupture of the crystal material. In addition, as Eq. (36) explicitly shows, a larger hot spot requires proportionally larger contact pressure and hence a much larger applied force (proportional to $r_0^3$).

A large applied force has several unwanted consequences. One is that the sampling is no longer nondestructive. A high contact force can damage or completely destroy the sample. Also, the sample morphology may change due to the high contact pressures and the chemical information thus obtained may be compromised. Independent of that, the mechanical support for the ATR element may flex in response to applied forces with effect on the optical alignment of the sampling accessory, resulting in an unwanted baseline shift and spurious spectral features due to the unequal optical paths between the sample and reference spectra, etc. Hence, it is beneficial to reduce the hot spot size to be as small as possible. However, the hot spot size reduction is optically coupled with the increase in the cone of the converging/diverging beam. The increase in the power of the incident beam means that the specificity in the angle of incidence is blurred. One can restore the angle of incidence definition by masking away the rays that fall outside the desired angular range, but at the expense of the light throughput and hence the $S/N$ ratio of the measurement.

### D. ATR in Process Control and Reaction Monitoring

The ability to monitor the changing chemical composition of a sample in real time makes IR spectroscopy useful for process control and reaction monitoring. ATR is particularly well suited to the task since it eliminates the need for a cell with a very short pathlength that would be required by transmission spectroscopy. A sensing ATR element could be built into the walls of the enclosing vessel and the monitoring could proceed without any interference with the process. Another method of interfacing the ATR sensor with the process is to attach the ATR sensor to a probe (usually a metal tube) and immersing the probe into the sample. Light could be transferred to the ATR element directly through the tube or through optical fibers. Regardless of how the light is transferred to the ATR element, the element has to be in direct physical contact with the sample. The conditions inside a chemical reactor could be extremely aggressive. High pressure, high/low temperatures, corrosive chemicals, etc. are not unusual within a chemical reactor. Not only must the ATR element itself be made to withstand these harsh conditions, but so do also the components employed to seal the ATR element into the probe. Fortunately, there are several materials commonly used to make ATR elements that are extremely chemically inert, mechanically strong, and thermally stable. Silicon, sapphire, and diamond are good examples. Sealing materials are also available. Teflon™ and Kalrez™ used as o-ring or gasket materials are fairly common. For higher temperatures (>250°C) metal seals are commonly used. The first such ATR probe that utilized a diamond ATR element, gold seal, and hastelloy probe body was described by Milosevic, Sting and Rein.[3] The probe is connected to an FTIR spectrometer via an articulated light conduit and inserted into a reaction vessel through a standard port. An alternative is a probe of a similar construction semi-permanently imbedded into the reaction vessel wall. These probes have been and continue to be successfully used in extremely corrosive environments and at the extremes of temperature and pressure.

### E. Grazing Angle ATR

Recently, a curious feature of ATR has resurfaced.[7] Under a certain set of conditions, ATR spectroscopy exhibits an extraordinary sensitivity to very thin films. In practical terms, the certain conditions referred to above are: a Ge ATR element, an ultra-thin film deposited onto a Si (or GaAs) wafer and the angle of incidence above critical (around 60°). An enhancement in the measured absorbance due to the sample, which is confined to the reflection of p-polarized light only, is roughly two orders of magnitude compared to

what would be obtained in a transmission experiment for the same sample. It is important to stress that this is not some new heretofore-undiscovered feature of the laws of reflection. This enhancement pops out of the familiar Fresnel formulae for reflectance. One simply needs to insert the appropriate values for the experimental parameters. This unusual phenomenon enables direct spectroscopic studies of films as thin as monolayers that are deposited on polished silicon wafers.

As long as the sample is much thinner than the wavelength of light used in the experiment, the sample's refractive index is immaterial. The critical angle is determined by the refractive indices of Ge ATR element and Si wafer. This angle is approximately 60°. Since a large angle of incidence is required, the technique has been named Grazing Angle ATR (GAATR). The sensitivity peaks near the critical angle and it decreases as the angle of incidence increases beyond critical. However, the incident angle has to be larger than critical for supercritical reflection needed for the ATR spectroscopy. Maximizing the sensitivity can thus be seen as making the angle of incidence as low as possible while still above critical.

Similar and in some respects related phenomenon[9] occurs if the silicon substrate is replaced with a metal such as gold. Although not internal reflection (since a metal has a higher refractive index than Ge), the phenomenon of enhanced sensitivity for an ultra-thin film on a metal surface shares with it the two important characteristics of GAATR: the experimental setup (equipment) and the extraordinary sensitivity. By employing the high refractive index material for the incident medium, the angle of incidence is effectively enhanced beyond grazing. Thus, the technique could be referred to as super-grazing angle reflection (SuGAR) spectroscopy. The same equipment (such as Harrick's GATR accessory) used to perform GAATR is used to perform SuGAR spectroscopy. As there is no critical angle, the sensitivity, in this case, increases with the increase in the angle of incidence. The sensitivity is still confined to the reflection of p-polarized light.

## IV. ACCESSORIES FOR ATR SPECTROSCOPY

Spectrometers, in general, are designed to collect spectra in transmission. The transmittance of a sample is defined as the ratio of the transmitted and the incident radiation. To measure a reflectance spectrum, the spectrometer alone does not suffice. An accessory is required to redirect the beam to and from the sample.

Reflection spectroscopy requires the beam path to be substantially different from that in transmission where it is a straight-line path. The function of the accessory is to correct for the increased path required by reflection

spectroscopy. Generally, the beam of the spectrometer is focused somewhere inside the sample compartment and the focal point is typically an image of the IR source. This source image is subsequently re-imaged onto the detector. Maximizing the signal-to-noise ratio (SNR) of the measurement requires the detector size to closely match that of the source image. Any defocusing of the IR beam causes the focus to occur either before or after the detector. The amount of light "seen" by the detector sharply decreases with the distance between the focal point and the detector. This defocusing inevitably leads to the deterioration in the SNR of the measurement and needs to be avoided.

This is illustrated in the Fig. 2. Here, the insertion of a multiple ATR accessory (in this case Harrick's Twin Parallel Mirror Attachment) does not change the way the IR beam is seen by the detector. The transfer of the focal point from the entrance aperture of the internal reflection element (IRE) to the exit aperture compensates for the increased pathlength of the IR beam in the sample compartment. In this case, what is imaged onto the detector is the exit aperture of the IRE rather than the IR source. The focal point transfer from the entrance to the exit of the IRE, originally introduced by Harrick,[2] is now almost universally used in conjunction with multiple reflection IREs.

Another, more frequently used method employs active optical components like powered mirrors or lenses. This method is illustrated in Fig. 3, where the two spherical mirrors compensate for the increased pathlength. The source image is re-imaged twice within the accessory. The first time, it is re-imaged onto the sampling surface of the hemispherical single reflection IRE. The second time, it is re-imaged into the position that is seen by the detector as the original place of the focal point in the sample compartment. Thus, the optical beam leaves the sample compartment as if the accessory was not present.

This being said, however, some degree of optical misalignment can be tolerated by the spectrometer without adversely affecting the quality of the

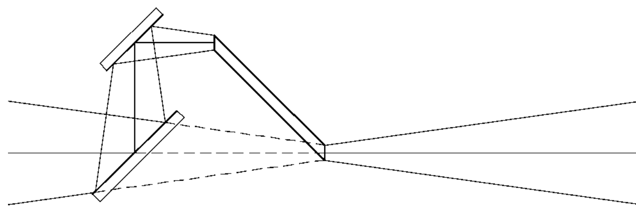

***Figure 2.*** Multiple ATR accessory.

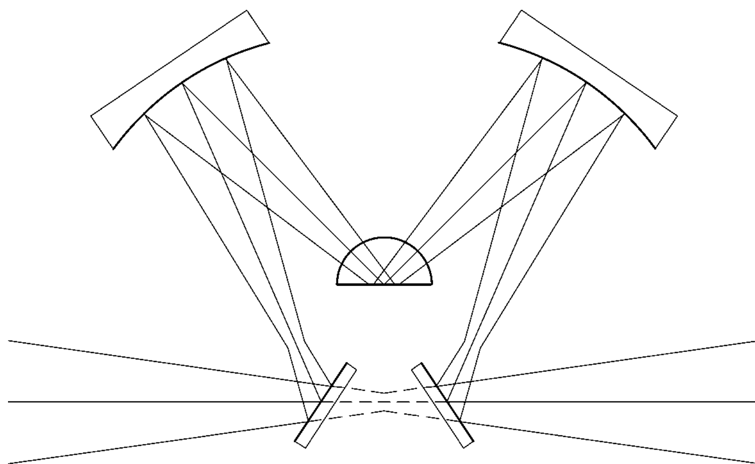

*Figure 3.* Single reflection ATR accessory.

measurement. The key point to this is that the misalignment leads to reduction in the strength of the signal on the detector. This reduction, if identical for the background and the sample spectra, while reducing the $S/N$ ratio of the measurement, does not change the reflectance values measured.

Many important issues arising from the geometry of the IREs, the angle of incidence, the reflectance of the entrance and exit apertures of the IREs, etc. have been discussed by Harrick.[2] An important variation of the multiple IRE geometry was introduced and discussed by Messerschmidt.[9] Harrick, Milosevic and Berets[10] introduced and discussed the concept of insensitive edges for the multiple IREs. Milosevic, Sting and Rein[6] introduced and discussed the concept of a wafer IRE where a large number of internal reflections occur within a circular area of only several millimeters in diameter.

Another area of development centered on single IREs. The single IREs were originally considered to be of somewhat narrow applicability. Limited $S/N$ performance of early spectrometers favored multiple reflection IREs. With advances in spectrometer performance and the shift in usage from research to industrial applications, the use of single reflection IREs increased dramatically. This shift was pioneered by Harrick's Prism Liquid Cell[11] accessory. The next advancement in single reflection ATR came with the introduction of Harrick's SplitPea[4] accessory and the ATR objective for IR microscopes.[5] Currently, the field of ATR spectroscopy is almost completely dominated by single reflection ATR accessories.

## V. CONCLUSION

The above review is far from being complete or exhaustive. It would be impossible to encompass, in a relatively short review paper, all the relevant aspects of this fascinating subject. Thus, it is necessary to choose topics that best reflect a particular point of view. The angle chosen here reflects my personal interests and fascinations. The emphasis in this paper is on the review of our understanding of the phenomenon of internal reflection as well as the associated phenomenon of the evanescent wave, and how these govern characteristics of ATR spectroscopy. I particularly wanted to stress the often glanced over differences between the two domains of internal reflection: the subcritical and the supercritical.

The machinery of electromagnetic theory was employed to discuss the advanced aspects of ATR spectroscopy. These aspects are rarely explicated and often given without adequate grounding in the basic electromagnetic theory. The aim here was to show how the vast diversity of the phenomena stems from, and is united by, the same well-known laws of electromagnetism.

## ACKNOWLEDGMENTS

I would like to thank my friend Hans (Bobby) Ulrich-Gremlich for encouragement and help with preparing this paper and many useful comments on the manuscript. Sue Berets read and provided helpful comments on the manuscript. Finally, I would like to acknowledge the enormous influence that N. J. Harrick, co-originator and the principal developer of ATR technique, had on my understanding of spectroscopy in general and ATR spectroscopy in particular.

## REFERENCES

1. (a) Born, M.; Wolf, E. *Principles of Optics*; Cambridge University Press: 1999; (b) Jackson, J.D. *Classical Electrodynamics*; Wiley: New York, 1998.
2. Harrick, N.J. *Internal Reflection Spectroscopy*; Wiley: New York, 1967.
3. Milosevic, M.; Harrick, N.J.; Berets, S.L. A multifunctional variable angle-reflection attachment. Appl. Spectrosc. **1991**, *45* (1), 126.
4. Harrick, N.J.; Milosevic, M.; Berets, S.L. Advances in optical spectroscopy: the ultra-small sample analyzer. Appl. Spectrosc. **1991**, *45* (6), 944.

5. Reffner, J.; Coates, J.; Messerschmidt, R.G. Chemical microscopy with FTIR microspectrometry. Am. Lab. **1987**, *86* (4).
6. Milosevic, M.; Sting, D.; Rein, A. Diamond-composite sensor for ATR spectroscopy. Spectroscopy **1995**, *10*, 44.
7. Milosevic, M.; Berets, S.L.; Fadeev, Y. Single reflection attenuated total reflection of organic monolayers on silicon. Appl. Spectrosc. **2003**, *57* (6), 4724.
8. Mulcahy, M.E.; Michl, J.; Berets, S.L.; Milosevic, M. Enhanced sensitivity in single-reflection spectroscopy of organic monolayers on metal substrates (pseudo-ATR). J. Phys. Chem. B **2004**, *108*.
9. Messerschmidt, R.G. A new internal reflection element design for high optical throughput in FT-IR. Appl. Spectrosc. **1986**, *40*, 632.
10. Harrick, N.J.; Milosevic, M.; Berets, S.L. New developments in internal reflection spectroscopy. Part II: The horizon. Am. Lab. **1992**, *24*, 29.
11. Harrick, N.J. Prism liquid cell. Appl. Spectrosc. **1983**, *37*, 573.